ORGANIC CHEMISTRY

Pd-catalyzed asymmetric Larock reaction for the atroposelective synthesis of N—N chiral indoles

Jinlei Wang[1], Deng Pan[2], Fen Wang[1], Songjie Yu[3]*, Genping Huang[2]*, Xingwei Li[1,3]*

Atropisomeric indoles defined by a N—N axis are an important class of heterocycles in synthetic and medicinal chemistry and material sciences. However, they remain heavily underexplored due to limited synthetic methods and challenging stereocontrol over the short N—N bonds. Here, we report highly atroposelective access to N—N axially chiral indoles via the asymmetric Larock reaction. This protocol leveraged the powerful role of chiral phosphoramidite ligand to attenuate the common ligand dissociation in the original Larock reaction, forming N—N chiral indoles with excellent functional group tolerance and high enantioselectivity via palladium-catalyzed intermolecular annulation between readily available *o*-iodoaniline and alkynes. The multifunctionality in the prepared chiral indoles allowed diverse post-coupling synthetic transformations, affording a broad array of functionalized chiral indoles. Experimental and computational studies have been conducted to explore the reaction mechanism, elucidating the enantio-determining and rate-limiting steps.

INTRODUCTION

The indole-based axially chiral platforms represent a privileged class of functional heterocycles (*1*–*4*). Consequently, catalytic and enantioselective synthesis of axially chiral indoles has become a highly important task in the past decades (*5*–*26*). In sharp contrast to the well-developed C—C or C—N axially chiral indole platforms, synthetic strategies to create indole-based biaryl scaffolds defined by a chiral N—N axis have remained in its infancy (*27*–*30*) due to the synthetic challenges associated with the steric hindrance imparted by a crowded chiral N—N axis. In addition, the N—N bond may also undergo cleavage due to its oxidizing nature. The enantioselective synthesis of N—N atropisomers remained elusive until very recently when the Lu/Houk and the Liu groups independently developed an *N*-allylic alkylation reaction (*31*) or desymmetrization of an existing pyrrole ring (*32*). Subsequently, increasing attention has been paid to two categories of asymmetric synthetic strategies in this regard, namely, late-stage functionalization (*33*–*38*) and de novo synthesis (*39*–*42*), for the expedient construction of indole-based N—N atropisomers that are known as unique and vital skeletons in bioactive molecules, organic materials, and chiral ligands (Fig. 1) (*43*–*46*). Recently, metal-catalyzed asymmetric peripheral C—H functionalization of *N*,*N*′-pyrrolylindoles has been independently disclosed by You and Liu toward synthesis of axially chiral N—N atropisomeric indoles (*47*–*48*), while the Li and Niu groups independently reported metal-catalyzed [4 + 2] annulation of amide substrates bearing a pre-existing indole ring to form N—N axially chiral indoles (*49*–*51*).

On the other hand, the de novo construction of an indole ring has also been recognized as an advantageous complement to the construction of N—N axially chiral indoles owing to the availability of substrates and synthetic modularity. In this context, Sparr and Wang independently accomplished Pd- or CPA-catalyzed atroposelective intramolecular hydroamination of *o*-alkynylanilines (Fig. 2A) (*52*–*53*). Soon after, Shi and colleagues ingeniously developed a CPA-catalyzed [3 + 2] de novo indolization, providing various axially chiral *N*,*N*′-bisindoles (*54*). More recently, Liu and colleagues disclosed the synthesis of N—N indole atropisomers via a sequence of condensation and palladium-catalyzed intramolecular *N*-arylation (*55*). Despite these elegant studies, note that these reported systems mostly suffered from intramolecular reactions, multiple manipulations, or limited substitution patterns. The investigations on direct approaches of metal-catalyzed enantioselective and intermolecular indolization remained rarely touched.

The rarity of intermolecular coupling systems in this context has called for the development of expedient synthetic methods. As a powerful solution to synthesize 2,3-disubstituted indoles, the Larock indolization reaction via palladium-catalyzed heteroannulation of *o*-iodoaniline with internal alkynes (Fig. 2B, top), reported in 1991 (*56*, *57*), attracted our attention. However, the atroposelective version of the Larock reaction remains untouched, even for the well-developed C—C or C—N axis (*58*). We envisaged that the well-tailored *N*-pyrrolyl-*o*-bromoaniline bearing steric demanding substituents on the pyrrole ring could serve as a promising substrate for the construction of N—N axial indoles via this asymmetric annulation strategy. To achieve this atroposelective system, the following three challenges should be addressed: (i) the fragile N—N bond in the substrate (193 kJ/mol) under harsh conditions (80° to 150°C), (ii) the strong background reaction in the absence of any ligand in the original Larock reaction, and (iii) the reduced enantiocontrol caused by a chiral ligand dissociation in the catalytic process. All these obstacles prompted us to develop a more efficient catalytic system beyond the original Larock indolization. While monodentate chiral phosphoramidites, privileged ligands in asymmetric catalysis (*59*–*62*), have been largely ignored in the Larock indole synthesis, they are powerful stronger π-acceptors than phosphine ligands with tunable donor properties by facile modification of the substituents at both the oxygen and the nitrogen atoms, as well as alignment of the dialkyl amine group with the phosphorus—metal bond via electronic interaction (*63*–*64*). These attractive properties inspired us to conceive of an efficient strategy in which phosphoramidites were explored as chiral ligands to achieve asymmetric Larock indolization (Fig. 2B, bottom). We now report our

[1]School of Chemistry and Chemical Engineering, Shaanxi Normal University (SNNU), Xi'an 710062, (China). [2]Department of Chemistry, School of Science and Tianjin Key Laboratory of Molecular Optoelectronic Sciences, Tianjin University, Tianjin 300072, (China). [3]Institute of Frontier Chemistry, School of Chemistry and Chemical Engineering, Shandong University, Qingdao 266237, (China).
*Corresponding author. Email: lixw@snnu.edu.cn (X.L.); gphuang@tju.edu.cn (G.H.); yusongjie23@sdu.edu.cn (S.Y.)

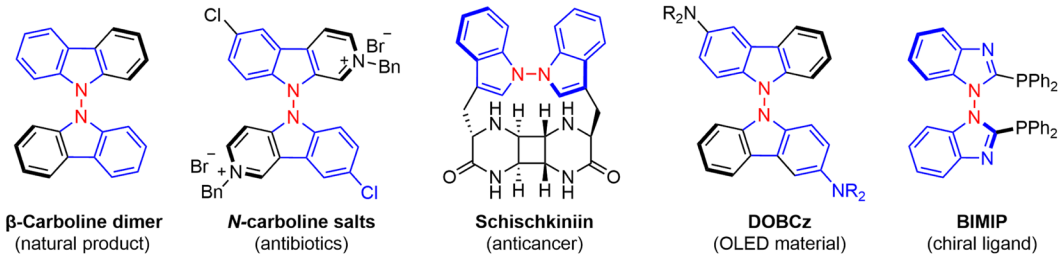

Fig. 1. Indole-based N—N atropisomers as functional molecules.

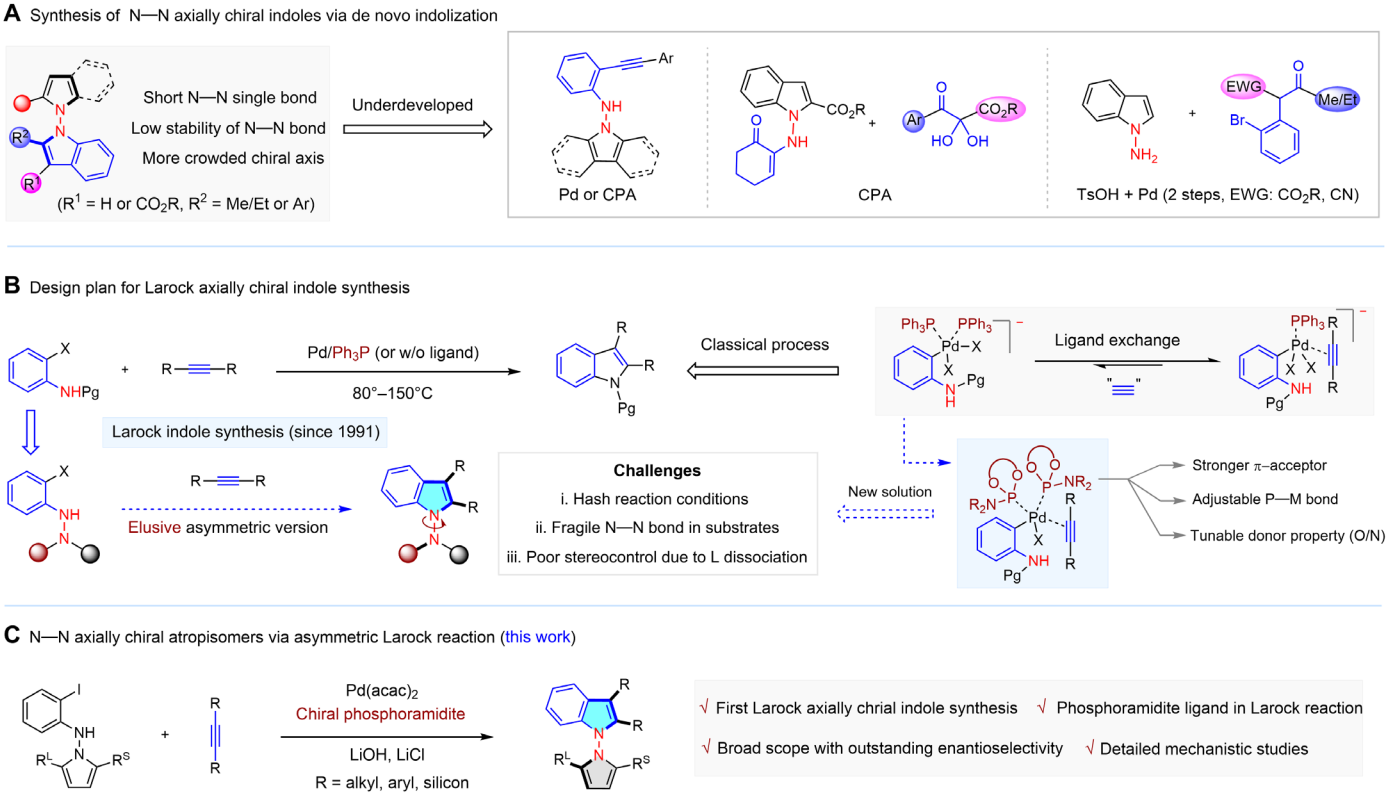

Fig. 2. Asymmetric synthesis of N—N axially chiral indoles and related challenges. (**A**) Synthesis of N—N axially chiral indoles via de novo indolization. (**B**) Design plan for Larock axially chiral indole synthesis. (**C**) N—N axially chiral atropisomers via asymmetric Larock reaction.

findings on a precisely designed asymmetric Larock indolization system for the atroposelective synthesis of N—N axially chiral indoles by the employment of a chiral monodentate phosphoramidite ligand instead of a commonly used monophosphine ligand (Fig. 2C).

RESULTS

Initial optimization studies

Our studies were initiated by investigation of palladium-catalyzed indolization between *N*-pyrrolyl-*o*-bromoaniline (**1a**) and diphenylacetylene (**2a**) in the presence of monophosphine ligands (**L1** and **L2**; Fig. 3), giving a good yield of the desired product **3** with rather low enantioselectivity. In contrast, bisphosphine ligands such as **L3** and **L4** all tend to exhibit poor reactivity, which is likely ascribed to the unfavorable dissociation of a phosphine arm from the palladium center to provide a vacant site for the π coordination. The desired coupling product **3** was still obtained in 20% yield in the absence of any ligand, demonstrating a background reaction in this coupling,

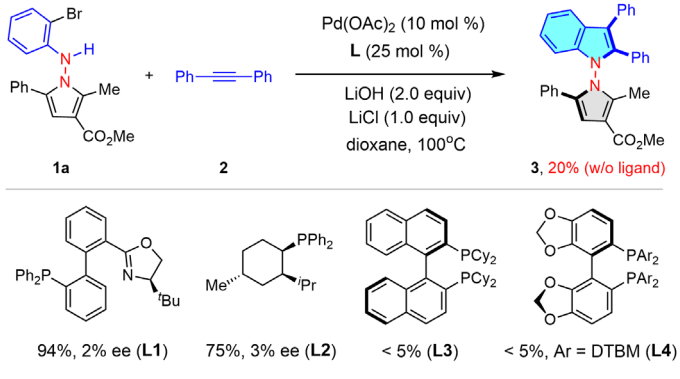

Fig. 3. Initial results for the asymmetric Larock indolization. Reactions were carried out using *N*-pyrrolyl-2-bromoaniline **1a** (0.05 mmol), diphenylacetylene **2a** (0.10 mmol), $Pd(OAc)_2$ (10 mol %), chiral ligand (P/Pd ratio = 2.5:1), base (2.0 equiv), 1,4-dioxane (1.0 ml), under N_2 at 100°C for 10 hours. ^{1}H nuclear magnetic resonance yield using 1,3,5-trimethoxybenzene as the internal standard.

which was also observed in previous Larock indole synthesis (*65*–*69*). The substantial challenges exemplified by the above preliminary outcomes called for the exploitation of another category of chiral ligands to achieve asymmetric Larock indolization.

To examine our hypothesis, we next performed detailed optimization of the same reaction using $Pd(OAc)_2$ as a catalyst and a chiral phosphoramidite ligand (Cs_2CO_3, 1,4-dioxane, 100°C; Table 1). A series of commercially available phosphoramidite ligands (**L5** to **L9**) were screened, all furnishing unsatisfactory outcomes in terms of efficiency and enantioselectivity (entries 1 and 2). Then, a SPINOL-based chiral phosphoramidite ligand **L10** was examined, affording product **3** in good yield and improved enantioselectivity (entry 3). Further comparisons with other analogous ligands **L11** to **L13** indicated the superiority of **L10** (entries 3 and 4). Examination of the base additive revealed that LiOH obviously outperformed others (entries 5 and 6). A series of palladium catalysts were next screened, and $Pd(acac)_2$ afforded enhanced enantioselectivity (entries 7 and 8). Encouragingly, good efficiency and enantioselectivity were maintained under a lower reaction temperature with a lower catalyst loading (6 mol %, entry 9). Further improvement of enantioselectivity was obtained by switching substrate **1a** to iodo analog **1b** (entry 10). The introduction of the LiCl additive slightly improved both the efficiency and enantioselectivity of the reaction (90% yield and 92% ee, entry 14).

Scope of internal acetylenes

The scope of the alkyne substrate was next explored by using *N*-pyrrolyl-*o*-iodoaniline **1b** as a substrate (Fig. 4). Symmetrical diarylacetylenes bearing electron-donating (alkyl and OMe), electron-withdrawing, and halogen substituents at the para position of benzene ring all reacted smoothly, providing the N─N atropisomers in consistently high yield and excellent enantioselectivity (**3** to **13**, 90 to 95% ee). Moreover, inclusions of alkyl, OMe, halogen, and CF_3 groups at the meta position of the benzene ring were also well-tolerated, affording products **14** to **17** with

Table 1. Optimization studies of a representative indolization system. Reaction conditions: *N*-pyrrolyl-2-haloaniline (0.05 mmol), diphenylacetylene (0.10 mmol), Pd catalyst (6 to 10 mol %), chiral ligand (L/Pd ratio = 2.5:1), base (2.0 equiv), additive (100 mol %), 1,4-dioxane (1.0 ml), under N_2 at 100°C for 10 hours.

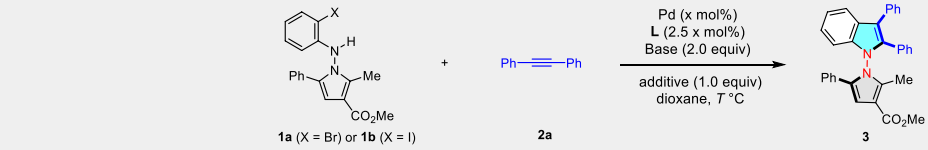

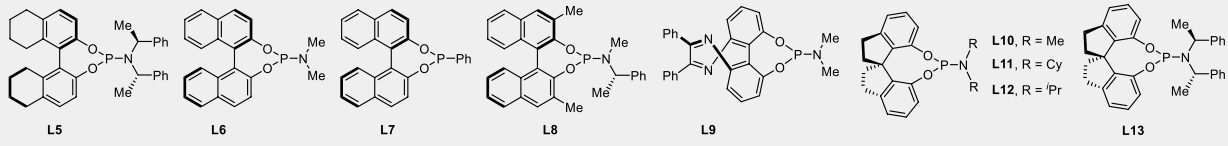

Entry	X	Catalyst (mol%)	L	Base	Additive	*T* (°C)	Yield (%)*	Ee (%)†
1	Br	$Pd(OAc)_2$ (10)	**L5**	Cs_2CO_3	-	100	28	2
2	Br	$Pd(OAc)_2$ (10)	**L6-9**	Cs_2CO_3	-	100	20-56	-16-6
3	Br	$Pd(OAc)_2$ (10)	**L10**	Cs_2CO_3	-	100	84	31
4	Br	$Pd(OAc)_2$ (10)	**L11-13**	Cs_2CO_3	-	100	23-65	8-17
5	Br	$Pd(OAc)_2$ (10)	**L10**	Na_3PO_4	-	100	81	49
6	Br	$Pd(OAc)_2$ (10)	**L10**	LiOH		100	85	78
7	Br	$Pd(acac)_2$ (10)	**L10**	LiOH		100	74	84
8	Br	$Pd(MeCN)_2Cl_2$ (10)	**L10**	LiOH		100	65	82
9‡	Br	$Pd(acac)_2$ (6)	**L10**	LiOH		85	92	88
10‡	I	$Pd(acac)_2$ (6)	**L10**	LiOH		85	78	90
11‡	I	$Pd(acac)_2$ (6)	**L10**	LiOH	LiCl	85	93	91
12‡	I	$Pd(acac)_2$ (6)	**L10**	LiOH	NaCl	85	87	89
13‡	I	$Pd(acac)_2$ (6)	**L10**	LiOH	NaI	85	62	89
14‡,§	I	$Pd(acac)_2$ (6)	**L10**	LiOH	LiCl	85	(90)	92

*^{1}H nuclear magnetic resonance yield using 1,3,5-trimethoxybenzene as the internal standard, isolated yield in parenthesis. †The ee was determined by high-performance liquid chromatography analysis. ‡18 hours. §The reaction mixture was stirred at room temperature for 10 min before heating.

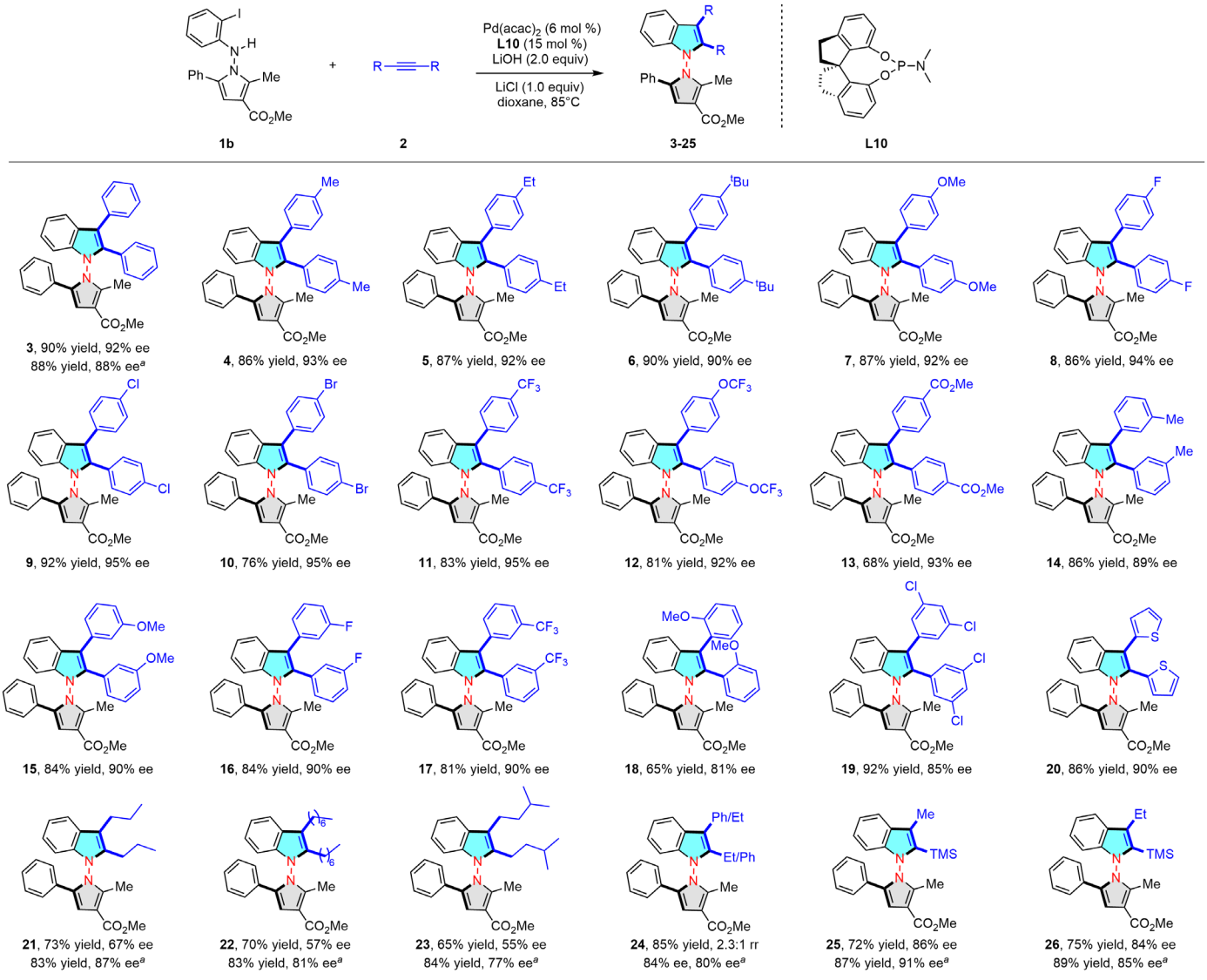

Fig. 4. Scope of alkynes in asymmetric Larock indolization. *N*-pyrrolyl-*o*-iodoaniline **1b** (0.10 mmol), diarylacetylene **2** (0.20 mmol), $Pd(acac)_2$ (6 mol %), **L10** (15 mol %), LiOH (0.20 mmol), and LiCl (0.10 mmol) in dioxane (2 ml), 85°C, 18 hours, isolated yield. [a]Bromoarene **1a** (0.10 mmol) was used.

high efficiency (81 to 86% yield, 89 to 90% ee). An exception was observed for an ortho OMe-substituted alkyne, which exhibited attenuated efficiency and enantioselectivity (**18**, 65% yield, 81% ee), likely due to steric effect. Meanwhile, 3,5-disubstituted and heteroarene-based alkynes also reacted smoothly (**19** and **20**, 85 to 90% ee). A series of symmetrical dialkylacetylenes were also explored. In this case, the bromoarene substrate outperformed its iodo analog in terms of enantioselectivity, and overall, a slightly decreased enantioselectivity has been realized (**21** to **23**, 77 to 87% ee). An alkyl-aryl alkyne was also explored. While the coupling of this alkyne proceeded smoothly, the regioselectivity was somewhat low (**24**, 2.3:1 rr, 84% ee and 80% ee). Gratifyingly, extension to several silyl-alkyl alkynes met with no difficulty, providing the corresponding products in high enantioselectivity and excellent regioselectivity (**25** and **26**, >20:1 rr), and the regioselectivity agrees with that in Larock's original report (*56*). All these outcomes verified the broad generality of the alkyne substrate.

Scope of *N*-pyrrolyl-*o*-iodoaniline

The scope of the *N*-pyrrolyl-*o*-iodoaniline was next investigated with diphenylacetylene as the coupling partner (Fig. 5). As expected, presence of alkyl, methoxy, phenyl, halogen, and ester groups at the four-position of the pyrrole-attached phenyl ring is well tolerated, which was evidenced by isolation of products **27** to **35** in high enantioselectivity (89 to 92% ee). Of note, the presence of a strong electron-withdrawing group (NO_2 and CN) had only marginal influence (**36** and **37**, 84 to 85% yield and 88 to 89% ee). Pyrrole substrates with 2-naphthyl, 3-substituted-, 4-substituted-, and 3,4-disubstituted phenyl groups all reacted smoothly, affording the products **38** to **44** in high enantioselectivity (85 to 93% ee). Besides, those with a 2-thienyl group or even a bulky tertiary alkyl group ortho to the chiral axis all coupled smoothly (**45** to **47**). Extension to other ester functionalities on the pyrrole ring expressed no evident effect on the efficiency and atroposelectivity (**48** to **52**). The absolute configuration of **48** was established by x-ray

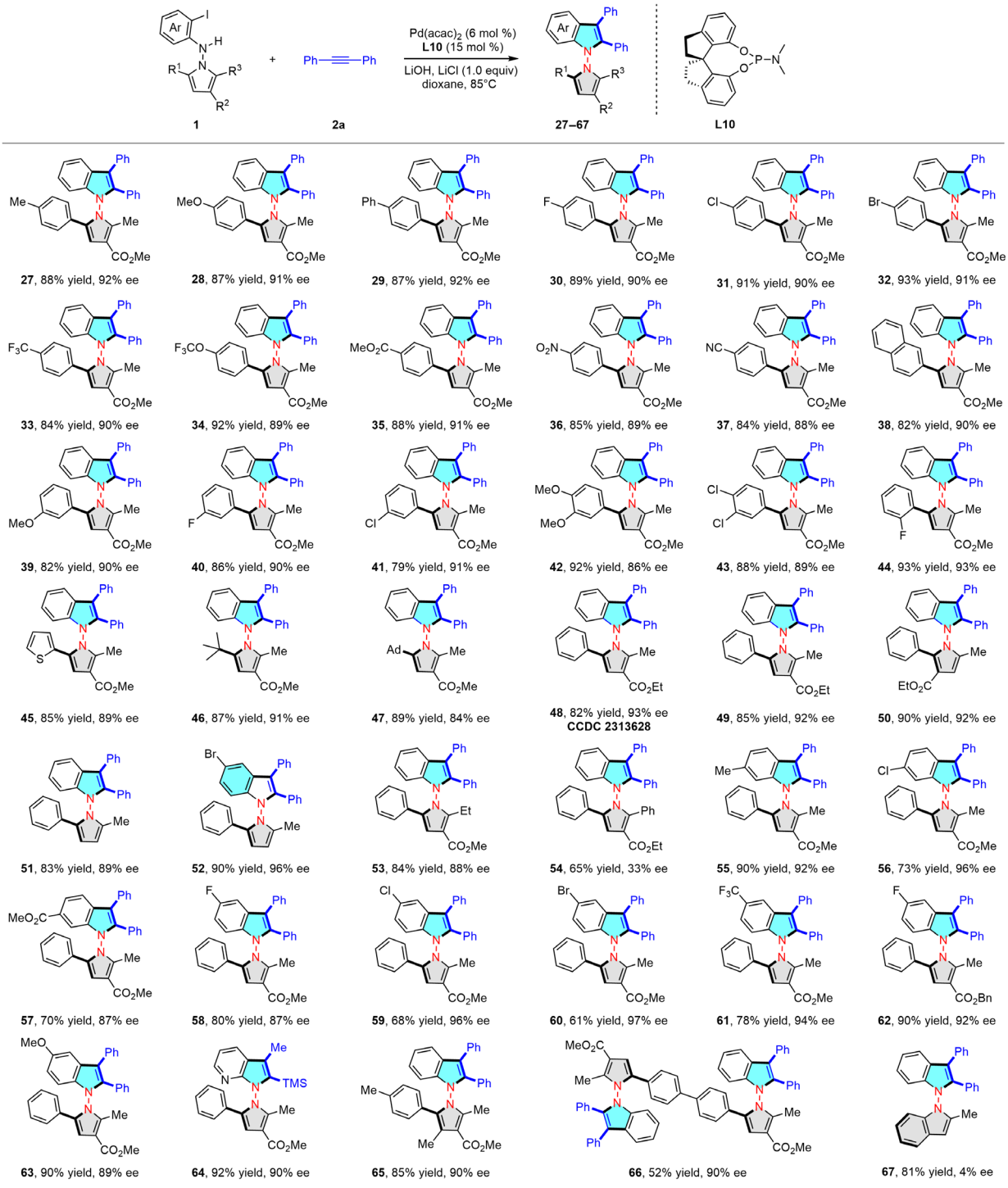

Fig. 5. Scope of *N*-pyrrolyl-*o*-iodoaniline in asymmetric Larock indolization. Reaction conditions: **1** (0.10 mmol), **2a** (0.20 mmol), $Pd(acac)_2$ (6 mol %), **L10** (15 mol %) LiOH (0.20 mmol), and LiCl (0.10 mmol) in 1,4-dioxane (2 ml), 85°C, 18 hours, isolated yield.

crystallographic analysis (**CCDC 2313628**). Replacing the methyl group on the indole ring with a bulkier one tends to give lower enantioselectivity (**53** and **54**), likely due to less steric bias of the two groups along the chiral axis. Moreover, comparable yield and enantioselectivity were also achieved for a series of substituted iodoaniline (**55** to **63**, 87 to 96% ee). Extension of the iodoaniline to a heteroaryl one also proved successful (**64**, 90% ee). The viability of a fully substituted pyrrole ring was also explored, and the corresponding product **65** was obtained in excellent enantioselectivity (90% ee). The coupling of a bispyrrole tethered by biphenylene afforded the distal N—N diaxes (**66**) in good yield with high atropo- and diastereoselectivity. In contrast, a nearly racemic product was observed for an indolyl-*o*-iodoaniline reagent (**67**), even

though the rotational barrier was calculated to be 43.3 kcal/mol. Thus, this negative result was presumably due to the loss of atroposelective control caused by the introduction of the fused phenyl ring [vide infra for density functional theory (DFT) rationalization].

Synthetic applications

Synthetic transformations of selected products were subsequently investigated. Two-gram–scale reactions by using both aryl iodides **1b** and **1y** proceeded efficiently in the coupling with diphenylacetylene (Fig. 6A), and the corresponding products **3** and **50** were isolated in excellent yield and enantioselectivity. The multifunctionality in the products allowed facile derivatization (Fig. 6B). Selective bromination of **3** with N-Bromosuccinimide (NBS) afforded product **68** in 95% yield, which was further transformed into **69** through the Suzuki coupling with 4-(9H-carbazol-9-yl)phenylboronic acid. Reduction of **3** by $LiAlH_4$ led to the formation of a primary alcohol **70**

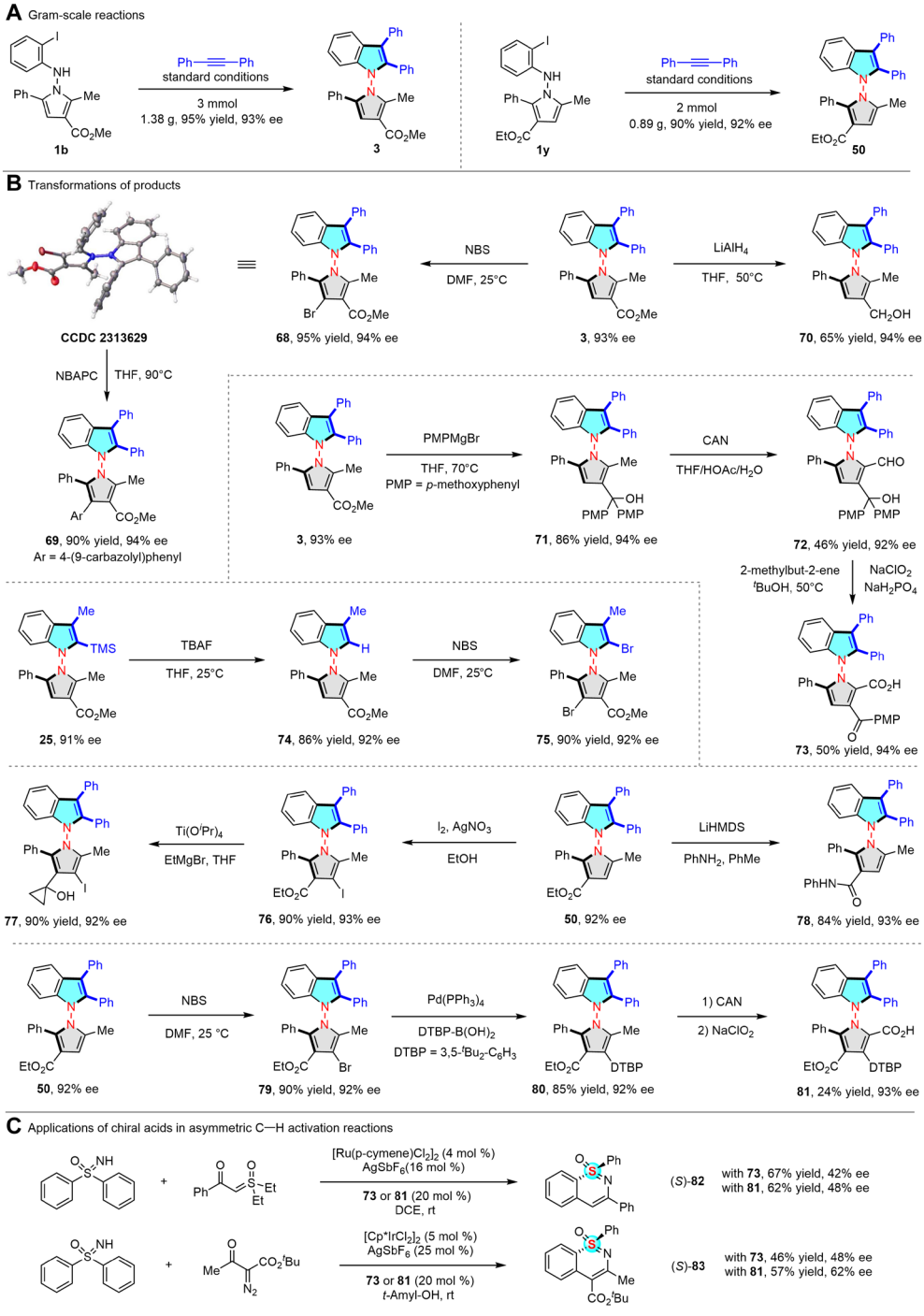

Fig. 6. Synthetic applications of selected products. (**A**) Gram-scale reactions. (**B**) Transformations of products. (**C**) Applications of chiral acids in asymmetric C—H activation reactions.

in 65% yield. The nucleophilic addition of a Grignard reagent to the ester group of **3** delivered tertiary alcohol **71** in 86% yield. Oxidation of **71** by CAN afforded a valuable aldehyde **72**, further oxidation of which gave a chiral carboxylic acid **73**. Moreover, the desilylation of product **25** afforded product **74** in 86% yield, which could be further dibrominated with NBS to afford product **75**. In addition, treatment of **50** with $I_2/AgNO_3$ produced the 3-iodo product **76**, which could be converted into product **77** through a Kulinkovich cyclopropanation. Moreover, aminolysis of **50** with an aniline generated the amide **78** in 84% yield. In all cases, the N—N axially chiral indole–based biaryl products were accessed with no erosion of enantiopurity. The applications of selected derivatized products have been also demonstrated in asymmetric catalysis (Fig. 6C). Enantioenriched carboxylic acid **73** was initially evaluated as a chiral additive in metal-catalyzed desymmetrizative annulation between sulfoximine and a carbene precursor such as sulfoxonium ylide or diazo reagent (*70*–*72*). The corresponding sulfur-stereogenic sulfoximines were obtained in moderate enantioselectivity (**82**, 42% ee; **83**, 48% ee). Considering the general trend that sterically hindered groups may exert high stereocontrol, a bulkier chiral acid **81** was prepared from **50** by following the same route via intermediates **79** and **80** (Fig. 6B). The employment of chiral acid **81** led to improved enantioselectivities for both catalytic reactions (**82**, 48% ee; **83**, 62% ee). These results demonstrated the synthetic potentials of our N—N axially chiral backbones. We also attempted to experimentally determine the configurational stability of the product **3**. No erosion of enantiopurity was observed after prolonged heating in mesitylene (130°C). DFT studies indicated a markedly high barrier (44.8 kcal/mol) for the rotation along the N—N axis, which is in line with related reports (*39*–*40*).

To better explore the values of our products, the bioactivities of our N—N axially heterobiaryl scaffolds were next investigated. The cytotoxicity of a representative compound **25** derived from a TMS-substituted alkyne was evaluated against several cancer cells such as hCG and Michigan Cancer Foundation-7 (MCF-7) (see the Supplementary Materials). Preliminary evaluation indicated that this compound exhibited a noticeable cell inhibitory rate (IC_{50} = 53.4 μM for hCG and IC_{50} = 71.6 μM for MCF-7) in anticancer activities at the micromolar level, indicating their promising applications in medicinal chemistry.

To clarify the role of chiral phosphoramidite ligand **L10** in the Larock indolization reaction, the nonlinear effect (NLE) of this chiral ligand has been investigated in the coupling of **1b** and **2a** (Fig. 7A). A negative NLE was observed in this system, suggesting that the palladium species involved in the enantio-determining step is likely stabilized by ≥ two **L10** ligands. In addition, the enantioselectivity of this coupling reaction varies with the **L10/Pd** ratio (Fig. 7B). An initial increase of ee with the **L10/Pd** ratio was found for product **3**, and saturation behavior was then observed with **L10/Pd** ≥ 2.5. This seems to suggest reversible ligation of the second chiral ligand **L10**. In line with this observation, higher enantioselectivity was observed when the reaction was carried out in a more concentrated solution (Fig. 7C). Collectively, all these data support that the Pd(II) species that undergo enantio-determining steps likely bear two chiral phosphine ligands [**Pd**(**L10**)$_2$], one of which is more prone to dissociation to give a monoligated species that competitively participates in enantio-determining step with attenuated enantioselectivity. Last, kinetic studies have been conducted to probe the rate-determining step (Fig. 7, D to F). The reaction is in zeroth order with respect to both substrates **1b** and **2a** and is a first-order dependence for the palladium catalyst, suggesting that the C—N reductive elimination is the rate-limiting step. Further mechanistic details of this coupling system were then elucidated by computational studies.

DFT calculations have been performed at the PBE0-D3BJ$_{(CPCM)}$/def2-TZVPP//B3LYP-D3(BJ)/SDD&6-31G(*d*) level of theory (see the Supplementary Materials for details). *N*-Pyrrolyl-*o*-iodoaniline **1b** and diphenylacetylene **2a** were selected as the model substrates. According to the experimental mechanistic studies (Fig. 8), both bisligated and monoligated reaction pathways have been evaluated. The monoligated pathway bears a higher barrier of C-I oxidative addition following the substitution of a chiral phosphine ligand by **2a**, which agrees with experimental studies that suggest the involvement of two

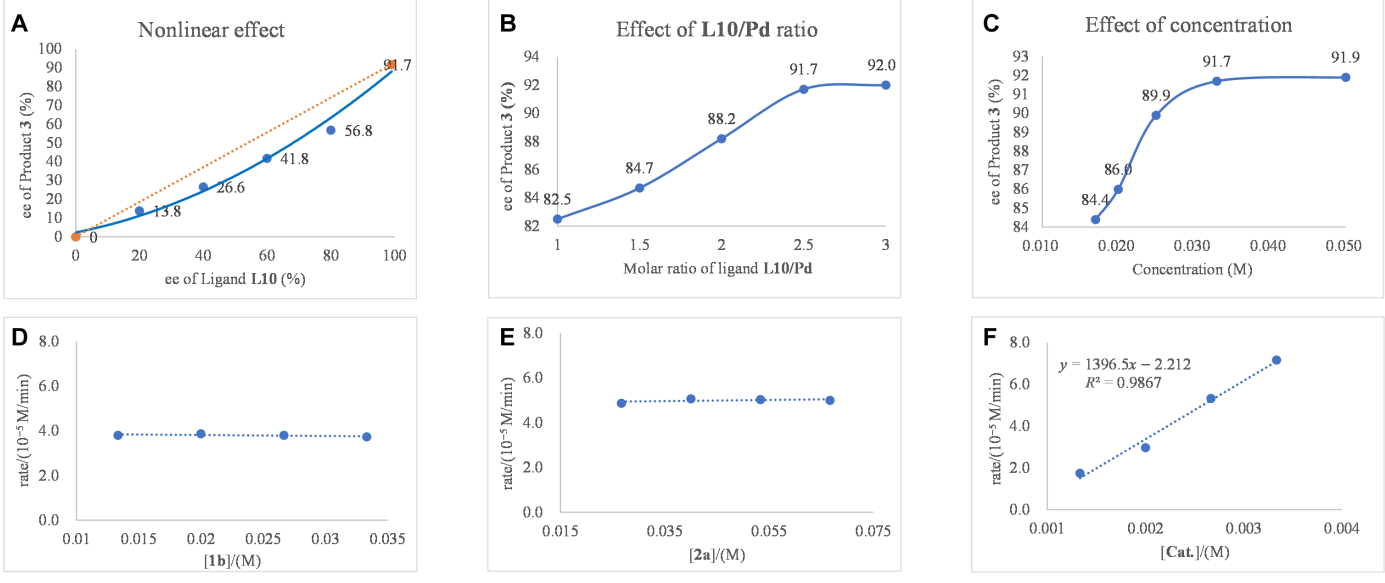

Fig. 7. Mechanistic studies of coupling of 1b and 2a. (**A**) Nonlinear effect of the ligand **L10**. (**B**) Effect of the **L10**/Pd ratio on the enantioselectivity. (**C**) Effect of concentration on the enantioselectivity. (**D**) Zeroth-order dependence of **1b**. (**E**) Zeroth-order dependence of alkyne **2**. (**F**) First-order dependence of the Pd catalyst.

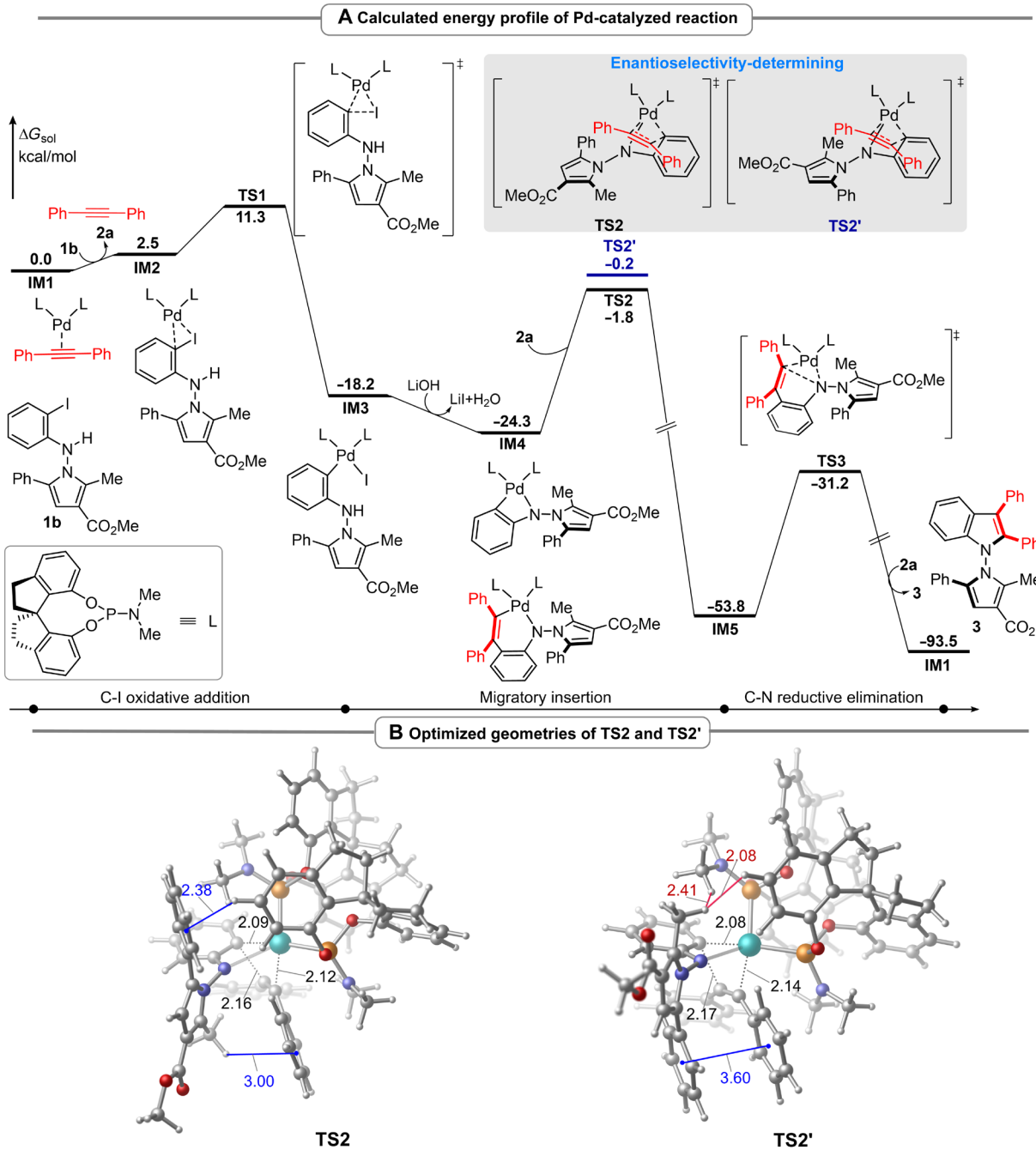

Fig. 8. Computational studies. (**A**) Calculated energy profile of the bisligated reaction pathway leading to desired product **3**. (**B**) Optimized geometries of the enantioselectivity-determining migratory insertion transition states. Bond distances are given in angstrom.

chiral phosphine ligands. For clarity, only the bisligated pathway is discussed in the main text (Fig. 8A), while the results of the monoligated pathway are provided in the Supplementary Materials. Our DFT studies commence with the ligand exchange between the alkyne-coordinated Pd(0) complex **IM1** and *N*-pyrrolyl-*o*-iodoaniline **1b**, leading to intermediate **IM2**. Subsequently, the C-I oxidative addition takes place through the transition state **TS1**. This step is highly exergonic, and the resulting Pd(II)-intermediate **IM3** is more stable than **IM2** by as much as 20.7 kcal/mol. The ensuing insertion of alkyne into the Pd—C bond was evaluated, and the removal of HI must occur with the assistance of the base additive LiOH, giving rise to the four-membered palladacycle **IM4**. Then, the migratory insertion of incoming alkyne **2a** into the Pd—C bond occurs via transition state **TS2**, resulting in intermediate **IM5**. Last, the catalytic cycle is completed by the C—N reductive elimination via transition state **TS3**, which would deliver the desired product **3** and regenerate the intermediate **IM1**.

The computations show that the C—N reductive elimination is the rate-determining step of the overall reaction, consistent with our kinetic studies. The enantioselectivity is determined by the migratory insertion step. The transition state **TS2** is lower in energy than **TS2′** by 1.6 kcal/mol (−1.8 versus −0.2 kcal/mol), in accordance with the experimentally observed enantioselectivity. Scrutiny of the optimized geometries reveals the presence of multiple noncovalent interactions (i.e., C—H…π and π…π) in **TS2** and **TS2′** (Fig. 8). However, the steric repulsion between the Me group of the *N*-pyrrolyl-*o*-iodoaniline moiety and the chiral ligand was observed in **TS2′** (2.08 and 2.41 Å), which is absent in **TS2**, thereby rendering **TS2′** higher in energy than **TS2**. [To be noted, the energy difference of the migratory insertion in the mono-ligated phosphine pathway was also examined (see the Supporting Material for details), and a smaller $\Delta\Delta G^{\neq} = 1.2$ kcal/mol was identified, which agrees with our experimental conclusions drawn from Figure 8.] In addition, we also scrutinized the poor enantioselectivity of product **67** by the same modeling. A much lower $\Delta\Delta G^{\neq}$ (0.5 kcal/mol) has been identified, which is in line with our experimentally observed low enantioselectivity (see Fig. 5 and the Supplementary Material for details).

DISCUSSION

We have developed the asymmetric Larock indole synthesis by employment of chiral phosphoramidite ligands to achieve the atroposelective construction of N—N axially chiral indoles. The indole ring in the atropisomeric product was constructed via a Pd-catalyzed annulation between readily available *N*-pyrrolyl-*o*-iodoaniline and internal alkynes. The reactions proceeded in high efficiency and enantioselectivity and exhibited a broad substrate scope and functional group compatibility. In addition, synthetic transformations of the products delivered various functionalized N—N axially chiral indole–based biaryls with multifunctionalities, which greatly expanded the arsenal of the underrepresented but important class of N—N atropisomers. Representative derivatized products have been demonstrated as a potential chiral additive in asymmetric C—H activation reactions. Therefore, this study not only unveiled an efficient asymmetric Larock indolization system but also provided a de novo entry to N—N axially chiral indole rings to add new members to the important family of the N—N atropisomers with synthetic and, possibly, biological applications.

MATERIALS AND METHODS

Synthesis of 3 to 66

Under N_2 atmosphere, $Pd(acac)_2$ (6 mol %), LiOH (2 equiv), *N*-aryl-2-haloaniline **1** (0.1 mmol), and alkyne **2** (2.0 equiv) were added to an oven-dried 10-ml sealed tube equipped with a stir bar. Then, chiral ligand **L10** (15 mol %) was dissolved in 1.0 ml of 1,4-dioxane in a separate tube and then transferred to the first one, followed by rinsing with an additional 0.50 ml of 1,4-dioxane. After stirring at the indicated temperature for 18 hours (monitored by thin-layer chromatography), the reaction mixture was diluted with EtOAc, filtered, and concentrated. The crude residue was purified by flash chromatography on silica gel using ethyl acetate and hexane (20:1 to 15:1) as the eluent to afford the desired products **3** to **66**.

Supplementary Materials

This PDF file includes:

Supplementary Text
Figs. S1 to S24
Tables S1 to S9
References

REFERENCES AND NOTES

1. G. R. Humphrey, J. T. Kuethe, Practical methodologies for the synthesis of indoles. *Chem. Rev.* **106**, 2875–2911 (2006).
2. A. J. Kochanowska-Karamyan, M. T. Hamann, Marine indole alkaloids: Potential new drug leads for the control of depression and anxiety. *Chem. Rev.* **110**, 4489–4497 (2010).
3. M. Inman, C. J. Moody, Indole synthesis–something old, something new. *Chem. Sci.* **4**, 29–41 (2013).
4. J. S. S. Neto, G. Zeni, Recent advances in the synthesis of indoles from alkynes and nitrogen sources. *Org. Chem. Front.* **7**, 155–210 (2020).
5. Z.-X. Zhang, T.-Y. Zhai, L.-W. Ye, Synthesis of axially chiral compounds through catalytic asymmetric reactions of alkynes. *Chem. Catal.* **1**, 1378–1412 (2021).
6. G.-J. Mei, W. L. Koay, C.-Y. Guan, Y. Lu, Atropisomers beyond the C–C axial chirality: Advances in catalytic asymmetric synthesis. *Chem* **8**, 1855–1893 (2022).
7. B.-M. Yang, X. Q. Ng, Y. Zhao, Enantioselective synthesis of indoles through catalytic indolization. *Chem Catal.* **2**, 3048–3076 (2022).
8. Y.-B. Wang, B. Tan, Construction of axially chiral compounds via asymmetric organocatalysis. *Acc. Chem. Res.* **51**, 534–547 (2018).
9. W. Qin, Y. Liu, H. Yan, Enantioselective synthesis of atropisomers via Vinylidene ortho-Quinone Methides (VQMs). *Acc. Chem. Res.* **55**, 2780–2795 (2022).
10. J. K. Cheng, S.-H. Xiang, B. Tan, Organocatalytic enantioselective synthesis of axially chiral molecules: Development of strategies and skeletons. *Acc. Chem. Res.* **55**, 2920–2937 (2022).
11. J. Kee Cheng, B. Tan, Chiral phosphoric acid-catalyzed enantioselective synthesis of axially chiral compounds involving indole derivatives. *Chem. Rec.* **23**, e202300147 (2023).
12. Y.-C. Zhang, F. Jiang, F. Shi, Organocatalytic asymmetric synthesis of indole-based chiral heterocycles: Strategies, reactions, and outreach. *Acc. Chem. Res.* **53**, 425–446 (2020).
13. H.-H. Zhang, F. Shi, Organocatalytic atroposelective synthesis of indole derivatives bearing axial chirality: Strategies and applications. *Acc. Chem. Res.* **55**, 2562–2580 (2022).
14. H.-H. Zhang, C.-S. Wang, C. Li, G.-J. Mei, Y. Li, F. Shi, Design and enantioselective construction of axially chiral naphthyl-indole skeletons. *Angew. Chem. Int. Ed.* **56**, 116–121 (2017).
15. C. Ma, F. Jiang, F.-T. Sheng, Y. Jiao, G.-J. Mei, F. Shi, Design and catalytic asymmetric construction of axially chiral 3,3′-bisindole skeletons. *Angew. Chem. Int. Ed.* **58**, 3014–3020 (2019).
16. F. Jiang, K.-W. Chen, P. Wu, Y.-C. Zhang, Y. Jiao, F. Shi, A strategy for synthesizing axially chiral naphthyl-indoles: Catalytic asymmetric addition reactions of racemic substrates. *Angew. Chem. Int. Ed.* **58**, 15104–15110 (2019).
17. L.-W. Qi, J.-H. Mao, J. Zhang, B. Tan, Organocatalytic asymmetric arylation of indoles enabled by azo groups. *Nat. Chem.* **10**, 58–64 (2018).
18. Q.-J. An, W. Xia, W.-Y. Ding, H.-H. Liu, S.-H. Xiang, Y.-B. Wang, G. Zhong, B. Tan, Nitrosobenzene-enabled chiral phosphoric acid catalyzed enantioselective construction of atropisomeric *N*-arylbenzimidazoles. *Angew. Chem. Int. Ed.* **60**, 24888–24893 (2021).
19. Z.-S. Wang, L.-J. Zhu, C.-T. Li, B.-Y. Liu, X. Hong, L.-W. Ye, Synthesis of axially chiral *N*-arylindoles via atroposelective cyclization of ynamides catalyzed by chiral brønsted acids. *Angew. Chem. Int. Ed.* **61**, e202201436 (2022).
20. H. Yang, H.-R. Sun, R.-Q. He, L. Yu, W. Hu, J. Chen, S. Yang, G.-G. Zhang, L. Zhou, Organocatalytic cycloaddition of alkynylindoles with azonaphthalenes for atroposelective construction of indole-based biaryls. *Nat. Commun.* **13**, 632 (2022).
21. Q. Ren, T. Cao, C. He, M. Yang, H. Liu, L. Wang, Highly atroposelective rhodium(II)-catalyzed N–H bond insertion: Access to axially chiral *N*-arylindolocarbazoles. *ACS Catal.* **11**, 6135–6140 (2021).
22. Y. Li, Y.-C. Liou, J. C. A. Oliveira, L. Ackermann, Ruthenium(II)/imidazolidine carboxylic acid-catalyzed C—H alkylation for central and axial double enantio-induction. *Angew. Chem. Int. Ed.* **61**, e202212595 (2022).
23. R. R. Surgenor, X. Liu, M. J. H. Keenlyside, W. Myers, M. D. Smith, Enantioselective synthesis of atropisomeric indoles via iron-catalysed oxidative cross-coupling. *Nat. Chem.* **15**, 357–365 (2023).
24. L.-W. Zhan, C.-J. Lu, J. Feng, R.-R. Liu, Atroposelective synthesis of C—N vinylindole atropisomers by palladium-catalyzed asymmetric hydroarylation of 1-alkynylindoles. *Angew. Chem. Int. Ed.* **62**, e202312930 (2023).
25. F.-T. Sheng, S. Yang, S.-F. Wu, Y.-C. Zhang, F. Shi, Catalytic asymmetric synthesis of axially chiral 3,3′-bisindoles by direct coupling of indole rings. *Chin. J. Chem.* **40**, 2151–2160 (2022).

26. Q.-Q. Hang, S.-F. Wu, S. Yang, X. Wang, Z. Zhong, Y.-C. Zhang, F. Shi, Design and catalytic atroposelective synthesis of axially chiral isochromenone-indoles. *Sci. China Chem.* **65**, 1929–1937 (2022).
27. T.-Y. Song, R. Li, L.-H. Huang, S.-K. Jia, G.-J. Mei, Catalytic asymmetric synthesis of N—N Atropisomers. *Chin. J. Org. Chem.* **43**, 1977–1990 (2023).
28. G. Centonze, C. Portolani, P. Righi, G. Bencivenni, Enantioselective strategies for the synthesis of N–N atropisomers. *Angew. Chem. Int. Ed.* **62**, e202303966 (2023).
29. J. Feng, R.-R. Liu, Catalytic asymmetric synthesis of N–N biaryl atropisomers. *Chem. A Eur. J.*, e202303165 (2023).
30. J. Feng, C.-J. Lu, R.-R. Liu, Catalytic asymmetric synthesis of atropisomers featuring an aza axis. *Acc. Chem. Res.* **56**, 2537–2554 (2023).
31. G.-J. Mei, J. J. Wong, W. Zheng, A. A. Nangia, K. N. Houk, Y. Lu, Rational design and atroposelective synthesis of N–N axially chiral compounds. *Chem* **7**, 2743–2757 (2021).
32. X.-M. Wang, P. Zhang, Q. Xu, C.-Q. Guo, D.-B. Zhang, C.-J. Lu, R.-R. Liu, Enantioselective synthesis of Nitrogen–nitrogen biaryl atropisomers via copper-catalyzed Friedel–Crafts alkylation reaction. *J. Am. Chem. Soc.* **143**, 15005–15010 (2021).
33. Q. Xu, H. Zhang, F.-B. Ge, X.-M. Wang, P. Zhang, C.-J. Lu, R.-R. Liu, Cu(I)-catalyzed asymmetric arylation of pyrroles with diaryliodonium salts toward the synthesis of N–N atropisomers. *Org. Lett.* **24**, 3138–3143 (2022).
34. W. Lin, Q. Zhao, Y. Li, M. Pan, C. Yang, G.-H. Yang, X. Li, Asymmetric synthesis of N–N axially chiral compounds via organocatalytic atroposelective N-acylation. *Chem. Sci.* **13**, 141–148 (2021).
35. C. Portolani, G. Centonze, S. Luciani, A. Pellegrini, P. Righi, A. Mazzanti, A. Ciogli, A. Sorato, G. Bencivenni, Synthesis of atropisomeric hydrazides by one-pot sequential enantio- and diastereoselective catalysis. *Angew. Chem. Int. Ed.* **61**, e202209895 (2022).
36. L.-Y. Pu, Y.-J. Zhang, W. Liu, F. Teng, Chiral phosphoric acid-catalyzed dual-ring formation for enantioselective construction of N–N axially chiral 3,3′-bisquinazolinones. *Chem. Commun.* **58**, 13131–13134 (2022).
37. M. Pan, Y.-B. Shao, Q. Zhao, X. Li, Asymmetric synthesis of N–N axially chiral compounds by phase-transfer-catalyzed alkylations. *Org. Lett.* **24**, 374–378 (2022).
38. J. Wang, X. Li, Rhodium-catalyzed enantio- and diastereoselective carboamidation of bicyclic olefins toward construction of remote chiral centers and axis. *Sci. China Chem.* **66**, 2046–2052 (2023).
39. K.-W. Chen, Z.-H. Chen, S. Yang, S.-F. Wu, Y.-C. Zhang, F. Shi, Organocatalytic atroposelective synthesis of N—N axially chiral indoles and pyrroles by de novo ring formation. *Angew. Chem. Int. Ed.* **61**, e202116829 (2022).
40. Y. Gao, L.-Y. Wang, T. Zhang, B.-M. Yang, Y. Zhao, Atroposelective synthesis of 1,1′-bipyrroles bearing a chiral N–N axis: Chiral phosphoric acid catalysis with lewis acid induced enantiodivergence. *Angew. Chem. Int. Ed.* **61**, e202200371 (2022).
41. Y. Wei, F. Sun, G. Li, S. Xu, M. Zhang, L. Hong, Enantioselective synthesis of N–N amide–pyrrole atropisomers via Paal–Knorr reaction. *Org. Lett.* **26**, 2343–2348 (2024).
42. Q. Huang, Y. Li, C. Yang, W. Wu, J. Hai, X. Li, Atroposelective synthesis of N–N axially chiral pyrrolyl(aza)-quinolinone by de novo ring formation. *Org. Chem. Front.* **11**, 726–734 (2024).
43. Z. Xu, M. Baunach, L. Ding, C. Hertweck, Bacterial synthesis of diverse indole terpene alkaloids by an unparalleled cyclization sequence. *Angew. Chem. Int. Ed.* **51**, 10293–10297 (2012).
44. B. R. Rosen, E. W. Werner, A. G. O'Brien, P. S. Baran, Total synthesis of dixiamycin B by electrochemical oxidation. *J. Am. Chem. Soc.* **136**, 5571–5574 (2014).
45. K. Suzuki, I. Nomura, M. Ninomiya, K. Tanaka, M. Koketsu, Synthesis and antimicrobial activity of β-carboline derivatives with N2-alkyl modifications. *Bioorg. Med. Chem. Lett.* **28**, 2976–2978 (2018).
46. X.-Y. Liu, Y.-L. Zhang, X. Fei, L.-S. Liao, J. Fan, 9,9′-Bicarbazole: New molecular skeleton for organic light-emitting diodes. *Chem. A Eur. J.* **25**, 4501–4508 (2019).
47. S.-Y. Yin, Q. Zhou, C.-X. Liu, Q. Gu, S.-L. You, Enantioselective synthesis of N—N biaryl atropisomers through iridium(I)-catalyzed C—H alkylation with acrylates. *Angew. Chem. Int. Ed.* **62**, e202305067 (2023).
48. W. Yao, C.-J. Lu, L.-W. Zhan, Y. Wu, J. Feng, R.-R. Liu, Enantioselective synthesis of N-N atropisomers by palladium-catalyzed C—H functionalization of pyrroles. *Angew. Chem. Int. Ed.* **62**, e202218871 (2023).
49. X. Zhu, H. Wu, Y. Wang, G. Huang, F. Wang, X. Li, Rhodium-catalyzed annulative approach to N–N axially chiral biaryls via C–H activation and dynamic kinetic transformation. *Chem. Sci.* **14**, 8564–8569 (2023).
50. Y. Wang, X. Zhu, D. Pan, J. Jing, F. Wang, R. Mi, G. Huang, X. Li, Rhodium-catalyzed enantioselective and diastereodivergent access to diaxially chiral heterocycles. *Nat. Commun.* **14**, 4661 (2023).
51. T. Li, L. Shi, X. Wang, C. Yang, D. Yang, M.-P. Song, J.-L. Niu, Cobalt-catalyzed atroposelective C—H activation/annulation to access N—N axially chiral frameworks. *Nat. Commun.* **14**, 5271 (2023).
52. V. Hutskalova, C. Sparr, Control over stereogenic N–N axes by Pd-catalyzed 5-endo-hydroaminocyclizations. *Synthesis* **55**, 1770–1782 (2023).
53. C.-S. Wang, Q. Xiong, H. Xu, H.-R. Yang, Y. Dang, X.-Q. Dong, C.-J. Wang, Organocatalytic atroposelective synthesis of axially chiral N,N′-pyrrolylindoles via de novo indole formation. *Chem. Sci.* **14**, 12091–12097 (2023).
54. Z.-H. Chen, T.-Z. Li, N.-Y. Wang, X.-F. Ma, S.-F. Ni, Y.-C. Zhang, F. Shi, Organocatalytic enantioselective synthesis of axially chiral N,N′-bisindoles. *Angew. Chem. Int. Ed.* **62**, e202300419 (2023).
55. P. Zhang, Q. Xu, X.-M. Wang, J. Feng, C.-J. Lu, Y. Li, R.-R. Liu, Enantioselective synthesis of N—N bisindole atropisomers. *Angew. Chem. Int. Ed.* **61**, 202212101 (2022).
56. R. C. Larock, E. K. Yum, Synthesis of indoles via palladium-catalyzed heteroannulation of internal alkynes. *J. Am. Chem. Soc.* **113**, 6689–6690 (1991).
57. R. C. Larock, E. K. Yum, M. D. Refvik, Synthesis of 2,3-disubstituted indoles via palladium-catalyzed annulation of internal alkynes. *J. Org. Chem.* **63**, 7652–7662 (1998).
58. G. Zhang, B. Yang, J. Yang, J. Zhang, Pd-catalyzed asymmetric larock indole synthesis to access axially chiral N-arylindoles. *J. Am. Chem. Soc.* **146**, 5493–5501 (2024).
59. A.-G. Hu, Y. Fu, J.-H. Xie, H. Zhou, L.-X. Wang, Q.-L. Zhou, Monodentate chiral spiro phosphoramidites: Efficient ligands for rhodium-catalyzed enantioselective hydrogenation of enamides. *Angew. Chem. Int. Ed.* **41**, 2348–2350 (2002).
60. B. L. Feringa, Phosphoramidites: Marvellous ligands in catalytic asymmetric conjugate addition. *Acc. Chem. Res.* **33**, 346–353 (2000).
61. J.-H. Xie, Q.-L. Zhou, Chiral diphosphine and monodentate phosphorus ligands on a spiro scaffold for transition-metal-catalyzed asymmetric reactions. *Acc. Chem. Res.* **41**, 581–593 (2008).
62. L. Eberhardt, D. Armspach, J. Harrowfield, D. Matt, BINOL-derived phosphoramidites in asymmetric hydrogenation: Can the presence of a functionality in the amino group influence the catalytic outcome? *Chem. Soc. Rev.* **37**, 839–864 (2008).
63. C. A. Tolman, Steric effects of phosphorus ligands in organometallic chemistry and homogeneous catalysis. *Chem. Rev.* **77**, 313–348 (1977).
64. J. F. Teichert, B. L. Feringa, Phosphoramidites: Privileged ligands in asymmetric catalysis. *Angew. Chem. Int. Ed.* **49**, 2486–2528 (2010).
65. G. Zeni, R. C. Larock, Synthesis of heterocycles via palladium-catalyzed oxidative addition. *Chem. Rev.* **106**, 4644–4680 (2006).
66. S. Cacchi, G. Fabrizi, Update 1 of: synthesis and functionalization of indoles through palladium-catalyzed reactions. *Chem. Rev.* **111**, PR215-PR283 (2011).
67. C.-Y. Chen, D. R. Lieberman, L. J. Street, A. R. Guiblin, R. D. Larsen, T. R. Verhoeven, An efficient synthesis of the indole acetic acid metabolite of MK-0462. *Synth. Commun.* **26**, 1977–1984 (1996).
68. N. Batail, A. Bendjeriou, T. Lomberget, R. Barret, V. Dufaud, L. Djakovitch, First heterogeneous ligand- and salt-free larock indole synthesis. *Adv. Synth. Catal.* **351**, 2055–2062 (2009).
69. N. Batail, V. Dufaud, L. Djakovitch, Larock heteroannulation of 2-bromoanilines with internal alkynes via ligand and salt free Pd/C catalysed reaction. *Tetrahedron Lett.* **52**, 1916–1918 (2011).
70. T. Zhou, P.-F. Qian, J.-Y. Li, Y.-B. Zhou, H.-C. Li, H.-Y. Chen, B.-F. Shi, Efficient synthesis of sulfur-stereogenic sulfoximines via Ru(II)-catalyzed enantioselective C–H functionalization enabled by chiral carboxylic acid. *J. Am. Chem. Soc.* **143**, 6810–6816 (2021).
71. J.-Y. Li, P.-P. Xie, T. Zhou, P.-F. Qian, Y.-B. Zhou, H.-C. Li, X. Hong, B.-F. Shi, Ir(III)-catalyzed asymmetric C–H activation/annulation of sulfoximines assisted by the hydrogen-bonding interaction. *ACS Catal.* **12**, 9083–9091 (2022).
72. L.-T. Huang, Y. Kitakawa, K. Yamada, F. Kamiyama, M. Kojima, T. Yoshino, S. Matsunaga, Enantioselective synthesis of 1,2-benzothiazine 1-imines via RuII/chiral carboxylic acid-catalyzed C—H alkylation/cyclization. *Angew. Chem. Int. Ed.* **62**, e202305480 (2023).
73. A. D. Becke, Density-functional thermochemistry. III. The role of exact exchange. *J. Chern. Phys.* **98**, 5648–5652 (1993).
74. S. Grimme, J. Antony, S. Ehrlich, H. Krieg, A consistent and accurate ab initio parametrization of density functional dispersion correction (DFT-D) for the 94 elements H-Pu. *J. Chem. Phys.* **132**, 154104 (2010).
75. D. Andrae, U. Häußermann, M. Dolg, H. Stoll, H. Preuß, Energy-adjustedab initio pseudopotentials for the second and third row transition elements. *Theor. Chem. Acc.* **77**, 123–141 (1990).
76. K. Fukui, Formulation of the reaction coordinate. *J. Phys. Chem.* **74**, 4161–4163 (1970).
77. K. Fukui, The path of chemical reactions - the IRC approach. *Acc. Chem. Res.* **14**, 363–368 (1981).
78. C. Adamo, V. Barone, Toward reliable density functional methods without adjustable parameters: The PBE0 model. *J. Chem. Phys.* **110**, 6158–6170 (1999).
79. S. Grimme, S. Ehrlich, L. Goerigk, Effect of the damping function in dispersion corrected density functional theory. *J. Comput. Chem.* **32**, 1456–1465 (2011).
80. F. Weigend, R. Ahlrichs, Balanced basis sets of split valence, triple zeta valence and quadruple zeta valence quality for H to Rn: Design and assessment of accuracy. *Phys. Chem. Chem. Phys.* **7**, 3297–3305 (2005).

81. F. Weigend, Accurate Coulomb-fitting basis sets for H to Rn. *Phys. Chem. Chem. Phys.* **8**, 1057–1065 (2006).
82. V. Barone, M. Cossi, Quantum calculation of molecular energies and energy gradients in solution by a conductor solvent model. *J. Phys. Chem. A* **102**, 1995–2001 (1998).
83. M. Cossi, N. Rega, G. Scalmani, V. Barone, Energies, structures, and electronic properties of molecules in solution with the C-PCM solvation model. *J. Comput. Chem.* **24**, 669–681 (2003).
84. G. Luchini, J. V. Alegre-Requena, I. Funes-Ardoiz, R. S. Paton, GoodVibes: Automated thermochemistry for heterogeneous computational chemistry data. *F1000Res* **9**, 291 (2020).
85. S. Grimme, C. Bannwarth, P. Shushkov, A robust and accurate tight-binding quantum chemical method for structures, vibrational frequencies, and noncovalent interactions of large molecular systems parametrized for all spd-block elements (Z = 1–86). *J. Chem. Theory Comput.* **13**, 1989–2009 (2017).
86. S. Grimme, C. Bannwarth, S. Dohm, A. Hansen, J. Pisarek, P. Pracht, J. Seibert, F. Neese, Fully automated quantum-chemistry-based computation of spin–Spin-coupled nuclear magnetic resonance spectra. *Angew. Chem. Int. Ed.* **56**, 14763–14769 (2017).
87. S. Grimme, Exploration of chemical compound, conformer, and reaction space with meta-dynamics simulations based on tight-binding quantum chemical calculations. *J. Chem. Theory Comput.* **15**, 2847–2862 (2019).
88. C. Bannwarth, S. Ehlert, S. Grimme, GFN2-xTB—An accurate and broadly parametrized self-consistent tight-binding quantum chemical method with multipole electrostatics and density-dependent dispersion contributions. *J. Chem. Theory Comput.* **15**, 1652–1671 (2019).

Acknowledgments: We thank J. Chang (Zhengzhou University) for biological studies. **Funding:** Financial support from the NSFC (nos. 22371175, 22101167, and 22073066), the Taishan Scholar of Shandong Province (20221108), and research fund from the SNNU is gratefully acknowledged. **Author contributions:** J.W. performed the experiments and analyzed the data. D.P. and G.H. performed the DFT calculations. J.W., S.Y., G.H., and X.L. designed and directed the project and wrote the manuscript. All authors discussed the results and commented on the manuscript. S.Y., G.H., and X.L. supported funding. **Competing interests:** The authors declare that they have no competing interests. **Data and materials availability:** All data needed to evaluate the conclusions in the paper are present in the paper and/or the Supplementary Materials.

Submitted 2 February 2024
Accepted 5 April 2024
Published 10 May 2024
10.1126/sciadv.ado4489